Intersection of Error Ellipsoids from at Least Two Positioning Sensors for Improved Sensor Fusion

Patrick Henkel, Medeea Horvat and Luka Sachße, *ANavS GmbH*

BIOGRAPHY

Patrick Henkel is the founder and managing director of ANavS and a senior lecturer at the Technical University of Munich (TUM), Germany. His research interests include all aspects of precise and reliable positioning. He lead the design of the reference PPP user algorithm for Galileo's new High Accuracy Service (HAS). He was a guest researcher at TU Delft in 2007, at the GPS Lab at Stanford University in 2008 and 2010, and at Curtin University in 2013. He received the Dissertation Award (2011) of the Vodafone Research Foundation for his PhD thesis on Precise Carrier Phase Positioning and was a Regional Winner in the European Satellite Navigation Competition (2010).

Medeea Horvat is currently pursuing a Master's degree in Mathematics at the Technical University of Munich (TUM), Germany. Her focus of studies is numerical analysis and scientific computing. She earned a Bachelor's degree in Mathematics and minored in Informatics at TUM (2020).

Luka Sachße is a software engineer in the ANavS Computer Vision Team. He graduated in 2019 at TUM from the Geodesy and Geoinformation master's program with a focus on Deep Learning based methods for Computer Vision and Remote Sensing. Since March 2020, he is working at ANavS where his main task is the integration of Visual SLAM / Odometry in the localization software of ANavS. For the SafeADArchitect research project, he coordinates the development of a risk-sensitive architecture for vehicle localization at ANavS.

ABSTRACT

Autonomous driving requires a precise and reliable positioning. A sensor fusion of multiple complementary sensors (e.g. Global Navigation Satellite System (GNSS) receivers, inertial sensors, odometry, camera, Lidar, Ultra-Wide Band) is typically performed to achieve the objectives of both high precision and high reliability.

A sensor fusion relies on an accurate knowledge of the measurement statistics. For static GNSS receivers, this assumption is typically well justified as multipath errors are only slowly changing with time. Henkel and Sperl (2016) and Henkel et al. (2016) showed that pseudorange multipath errors can be estimated as additional state parameters within the RTK and PPP solution. Unfortunately, an accurate knowledge of the measurement statistics is often not available for kinematic receivers in challenging environments: More specifically, the number of measurement epochs needed to estimate the measurement statistics is in urban environments often much larger than the number of epochs with equal statistics, e.g. a car can pass below a tree within one second, and thereby drive from an area with excellent satellite visibility via a severe multipath environment to another area with very good satellite visibility. This shows the need for a verification and adaption of the GNSS measurement statistics with the help of other sensors.

In this paper, we propose a method that checks the consistency of the error ellipsoids from different sensors by searching a common intersection point of all ellipsoids. We provide a general numerical approach as an analytical solution exists only for the intersection of two ellipsoids. The proposed method should be applied as part of the pre-processing to improve the statistics of the measurements from each sensor. We show that the proposed method is numerically very efficient, i.e. it can reduce the number of samples needed to find the intersection by up to two orders of magnitude compared to a brute-force search.

I. INTRODUCTION

A sensor fusion of GNSS RTK, INS, odometry and map matching is a popular approach for precise and reliable positioning for autonomous driving. A tight coupling can be efficiently performed by a Kalman filter as described in Brown and Hwang (2012). A typical challenge of the Kalman filter solution is that it underestimates the positioning accuracy. Typical reasons are time-correlated errors (e.g. multipath), modeling errors and erroneous measurement and/ or process noise covariance matrices. A Kalman filter propagates the statistics of the estimated states without using the measurements, i.e. it fully relies on a correct knowledge of the measurement and process noise covariance matrices, the measurement and state space model, and the initial uncertainty of the estimated states.

In this paper, we address the problem of imperfect knowledge of the statistics by checking the overlapping of the error ellipsoids from at least two positioning sensors. Our method determines the existence of a common intersection area from two, three or even more positioning sensors. We provide a numerical solution as an analytical one exists only for the intersection of two ellipsoids. The latter one has been studied in details by Kerr (1974), Alfano and Greer (2003), Duzak (2007) and Gilitschenski and Hanebeck (2012).

Fig. 1 visualizes our problem: Three error ellipsoids from three different positioning sensors have their individual centers, orientation and extension. The objective is to figure out, whether there exists or not exists a common intersection area of all ellipsoids.

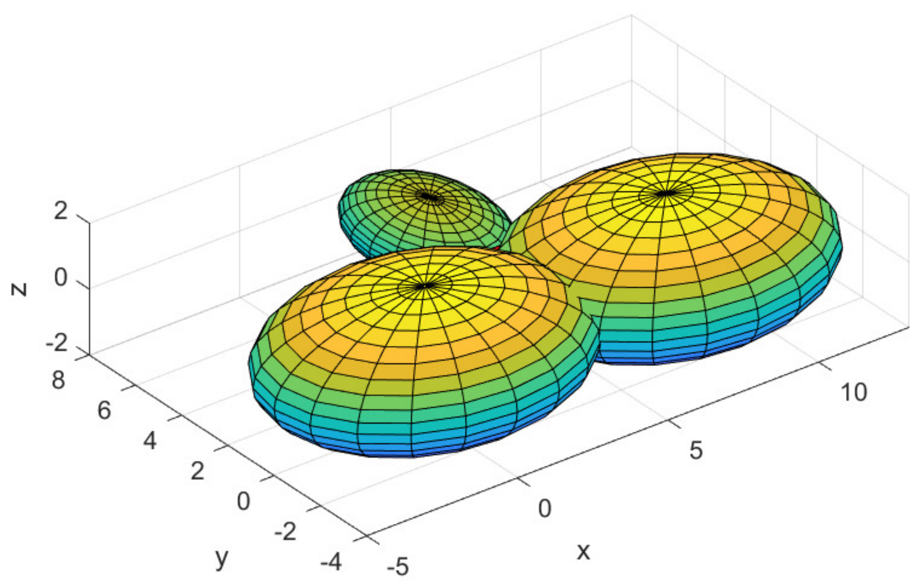

Figure 1: Error ellipsoids from three different positioning sensors. The objective of this paper is to provide an efficient method for checking the existence of a common intersection area.

This paper is organized as follows: In section II, we start with a probabilistic description of the position estimates from different sensors. In section III, we provide a mathematical formulation of our problem. The methodology for solving the problem is explained in section IV. The section is split into four sub-sections for the four steps of the method. Section V includes the results. A discussion of these results and our conclusion is provided in section VI.

II. PROBABILISTIC DESCRIPTION OF POSITIONING ESTIMATES

Every positioning sensor is affected by measurement noise, and this measurement noise is typically assumed to be Gaussian distributed. As the position estimate is typically three-dimensional, we describe it by a multi-dimensional Gaussian distribution:

$$f(\hat{x}_i) = \frac{1}{\sqrt{(2\pi)^k |\Sigma_{\hat{x}_i}|}} \cdot \exp\left((\hat{x}_i - \mu_i)^{\mathrm{T}} \, \Sigma_{\hat{x}_i}^{-1} \, (\hat{x}_i - \mu_i) \right), \tag{1}$$

where the index $i \in \{1, \ldots, s\}$ denotes the sensor (e.g. GNSS, INS, camera or LiDAR based Simultaneous Localization and Mapping Leonard and Durrant-Whyte (1991), Ulta-Wide Band based positioning), $\hat{x}_i$ describes its estimate, μ_i is the mean value, and $\Sigma_{\hat{x}_i}$ denotes the covariance matrix of the estimate. Obviously, an estimate $\hat{x}_i$ being close to μ_i is more likely than an estimate being far from μ_i. We solve Eq. (1) for the argument of the exponential function to obtain:

$$(\hat{x}_i - \mu_i)^{\mathrm{T}} \Sigma_{\hat{x}_i}^{-1} (\hat{x}_i - \mu_i) = \alpha \quad \text{with} \quad \alpha = \ln\left(\sqrt{(2\pi)^k |\Sigma_{\hat{x}_i}|} \cdot f(\hat{x}_i)\right). \tag{2}$$

which corresponds to the ellipsoid equation, whereas the probability $f(\hat{x}_i)$ controls the size of the ellipsoid. The cumulative probability of a position estimate being outside the error ellipsoid is obtained by integration of $f(\hat{x}_i)$ over the tail of the distribution. This probability can be reduced by increasing α.

III. PROBLEM STATEMENT

Our objective is to find out whether the error ellipsoids from $s \geq 2$ independent positioning sensors (e.g. GNSS RTK, INS, camera SLAM, LiDAR SLAM, UWB) have a common intersection. More specifically, we would like to check, whether there exists at least one point that completely fulfills the following set of ellipsoidal inequalities:

$$(x - \mu_i)^{\mathrm{T}} \Sigma_{\hat{x}_i}^{-1} (x - \mu_i) \leq 1 \quad \forall \quad i \in \{1, \ldots, s\}, \tag{3}$$

where x denotes the unknown position of a point within the intersection of all ellipsoids, μ_i denotes the known center of the ellipsoid, and $\Sigma_{\hat{x}_i}$ represents the related known covariance matrix. The outcome of the intended check is a simple binary information about the existence or not-existence of a common intersection.

There does exist an analytical solution for $s = 2$. However, we are not aware of any analytical solution for $s \geq 3$. The objective of this paper is to present a numerically efficient solution that can be used for any $s \geq 2$.

IV. METHODOLOGY FOR SOLVING PROBLEM STATEMENT

In this section, we present our methodlogy to solve the above problem in four steps: In the first step, we determine the eigenvectors and eigenvalues of the inverse state covariance matrices to charaterize the bounding boxes for each ellipsoid. The second step is the crucial one: A single tight rectangular bounding box is determined that includes the intersection area of all ellipsoids. The Simplex algorithm as described by Murty (2000) is used to solve a constrained optimization problem. In the third step, we compute samples from a uniform distribution within the single tight rectangular bounding box. Finally, we check whether a sample is within all ellipsoids.

1. Determination of eigenvectors and eigenvalues of inverse state covariance matrices

As a first step, we determine the eigenvectors and eigenvalues of the inverse covariance matrix $\Sigma_{\hat{x}_i}^{-1}$, i.e.

$$\Sigma_{\hat{x}_i}^{-1} = Q_i \Lambda_i Q_i^{\mathrm{T}} \tag{4}$$

with $Q_i = (q_{i,1}, q_{i,2}, q_{i,3})$ being the matrix of orthonormal eigenvectors and $\Lambda_i = \mathrm{diag}\,(\lambda_{1,i}, \lambda_{2,i}, \lambda_{3,i})$ being the diagonal matrix of eigenvalues. The orthnormal eigenvectors describe the orientation of the ellipsoids. The eigenvalues λ_i are related to the semi-major axes lengths a_i, b_i and c_i:

$$\lambda_{1,i} = \frac{1}{a_i^2}, \quad \lambda_{2,i} = \frac{1}{b_i^2}, \quad \lambda_{3,i} = \frac{1}{c_i^2}. \tag{5}$$

The eigenvectors and eigenvalues describe not only the ellipsoids but also their bounding boxes. More specifically, the bounding box of ellipsoid $i \in \{1, \ldots, s\}$ is defined by 6 inequalities:

$$Q_i^{\mathrm{T}} (x - \mu_i) \leq \begin{pmatrix} a_i \\ b_i \\ c_i \end{pmatrix} \qquad \text{and} \qquad Q_i^{\mathrm{T}} (x - \mu_i) \geq - \begin{pmatrix} a_i \\ b_i \\ c_i \end{pmatrix}, \tag{6}$$

where x denotes an arbitrary position within the bounding box or on its edge.

2. Determination of common tight rectangular bounding box for efficient sampling

As there does not exist an analytical solution for the determination of the intersection of three or more ellipsoids, one needs to perform a numerical sampling. One can sample the interior of each ellipsoid and check, whether there exists at least one sample that is within all ellipsoids. However, this approach is numerically very inefficient for moderate to large error ellipsoids.

Therefore, we reduce the volume to be sampled by determining a Common Tight Rectangular Bounding Box (CTRBB) of the ellipsoidal intersection area as shown in Fig. 2. We assume without loss of generality that the sides of the CTRBB are parallel to the basis vectors $e_1 = (0, 0, 1)^{\mathrm{T}}$, $e_2 = (0, 1, 0)\mathrm{T}$ and $e_3 = (0, 0, 1)^{\mathrm{T}}$ of our coordinate frame. The starting and ending point of the CTRBB along the axis e_j, $j \in \{1, 2, 3\}$, are defined by a minimization/ maximization criteria and the $6s$ inequality constraints of Eq. (6).

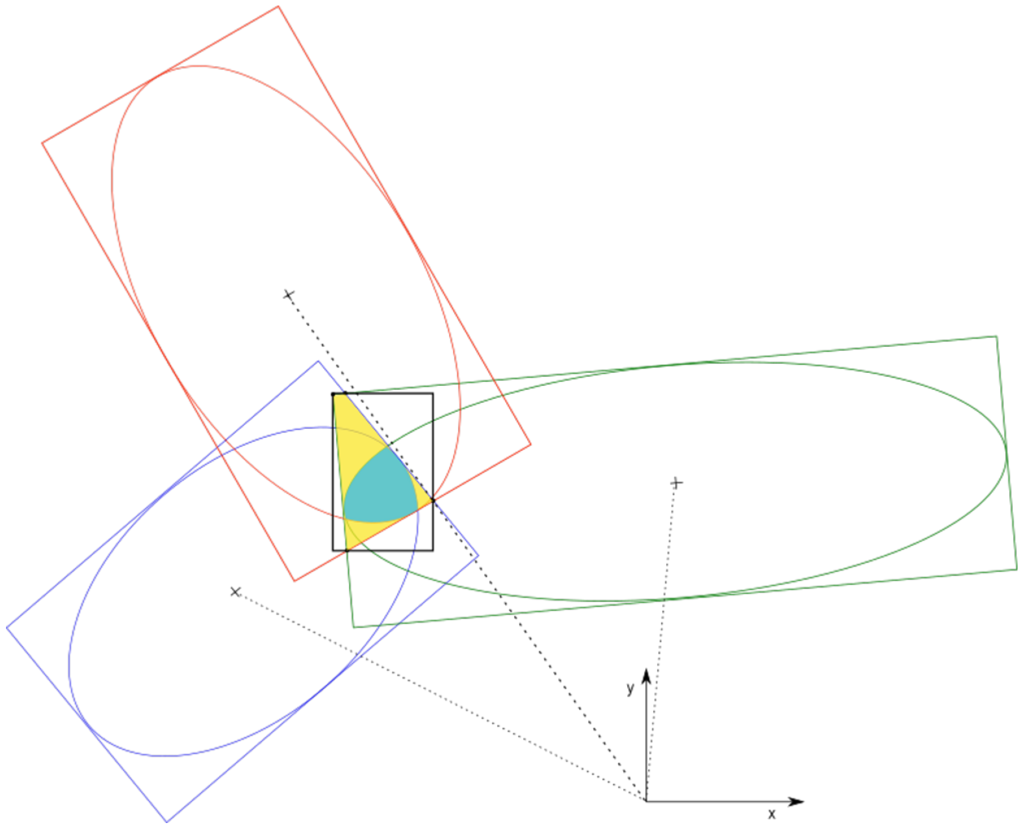

Figure 2: The intersection of the three error ellipses is shown in blue. Each individual ellipse is circumscribed by an individual bounding box. The yellow area describes the intersection of the individual bounding boxes and includes the blue area as subset. The yellow area can be described by linear border lines but the overall shape of it is no longer rectangular. Therefore, a Common Tight Rectangular Bounding Box (CTRBB, shown in bold black lines) is defined, which includes the yellow area (intersection of individual bounding boxes) and blue area (intersection of ellipsoids) as subsets.

Thus, the starting point of the CTRBB along e_1 is defined as:

$$\begin{aligned} x^- \quad &:= \quad \min_x \quad \left(e_1^{\mathrm{T}} x\right) \\ &\text{s.t.} \quad Q_i^{\mathrm{T}} (x - \mu_i) \geq - \begin{pmatrix} a_i \\ b_i \\ c_i \end{pmatrix} \quad \text{and} \quad Q_i^{\mathrm{T}} (x - \mu_i) \leq \begin{pmatrix} a_i \\ b_i \\ c_i \end{pmatrix} \quad \forall \quad i \in \{1, \ldots, s\}. \end{aligned} \tag{7}$$

The ending point of the CTRBB along e_1 is defined similarly as:

$$\begin{aligned} x^+ \quad &:= \quad \max_x \quad \left(e_1^{\mathrm{T}} x\right) \\ &\text{s.t.} \quad Q_i^{\mathrm{T}} (x - \mu_i) \geq - \begin{pmatrix} a_i \\ b_i \\ c_i \end{pmatrix} \quad \text{and} \quad Q_i^{\mathrm{T}} (x - \mu_i) \leq \begin{pmatrix} a_i \\ b_i \\ c_i \end{pmatrix} \quad \forall \quad i \in \{1, \ldots, s\}. \end{aligned} \tag{8}$$

In Fig. 2, the values x^- and x^+ describe the left and right edge of the CTRBB.

The starting and ending points of the other two sides of the CTRBB are defined accordingly:

$$\begin{aligned} y^- \quad &:= \quad \min_x \quad \left(e_2^{\mathrm{T}} x\right) \\ &\text{s.t.} \quad Q_i^{\mathrm{T}}\left(x-\mu_i\right) \geq -\begin{pmatrix} a_i \\ b_i \\ c_i \end{pmatrix} \quad \text{and} \quad Q_i^{\mathrm{T}}\left(x-\mu_i\right) \leq \begin{pmatrix} a_i \\ b_i \\ c_i \end{pmatrix} \quad \forall \quad i \in \{1, \ldots, s\}. \end{aligned} \tag{9}$$

$$\begin{aligned} y^+ \quad &:= \quad \max_x \quad \left(e_2^{\mathrm{T}} x\right) \\ &\text{s.t.} \quad Q_i^{\mathrm{T}}\left(x-\mu_i\right) \geq -\begin{pmatrix} a_i \\ b_i \\ c_i \end{pmatrix} \quad \text{and} \quad Q_i^{\mathrm{T}}\left(x-\mu_i\right) \leq \begin{pmatrix} a_i \\ b_i \\ c_i \end{pmatrix} \quad \forall \quad i \in \{1, \ldots, s\}. \end{aligned} \tag{10}$$

$$\begin{aligned} z^- \quad &:= \quad \min_x \quad \left(e_3^{\mathrm{T}} x\right) \\ &\text{s.t.} \quad Q_i^{\mathrm{T}}\left(x-\mu_i\right) \geq -\begin{pmatrix} a_i \\ b_i \\ c_i \end{pmatrix} \quad \text{and} \quad Q_i^{\mathrm{T}}\left(x-\mu_i\right) \leq \begin{pmatrix} a_i \\ b_i \\ c_i \end{pmatrix} \quad \forall \quad i \in \{1, \ldots, s\}. \end{aligned} \tag{11}$$

$$\begin{aligned} z^+ \quad &:= \quad \max_x \quad \left(e_3^{\mathrm{T}} x\right) \\ &\text{s.t.} \quad Q_i^{\mathrm{T}}\left(x-\mu_i\right) \geq -\begin{pmatrix} a_i \\ b_i \\ c_i \end{pmatrix} \quad \text{and} \quad Q_i^{\mathrm{T}}\left(x-\mu_i\right) \leq \begin{pmatrix} a_i \\ b_i \\ c_i \end{pmatrix} \quad \forall \quad i \in \{1, \ldots, s\}. \end{aligned} \tag{12}$$

We solve these constrained optimization problems with the famous **Simplex** algorithm described by Murty (2000). If the Simplex algorithm does not find a solution, we already know that there is no intersection between the error ellipsoids.

3. Generation of uniformly distributed samples in the common tight rectangular bounding box

In the previous step, we have determined the boundaries of the Common Tight Rectangular Bounding Box (CTRBB) that includes the ellipsoidal intersection area. In this step, we generate uniformly distributed samples $x_j = (x_{j,1}, x_{j,2}, x_{j,3})^{\mathrm{T}}$ that are within the CTRBB, i.e.

$$\begin{aligned} x_{j,1} &\sim \mathcal{U}\left(x^-, x^+\right) \\ x_{j,2} &\sim \mathcal{U}\left(y^-, y^+\right) \\ x_{j,3} &\sim \mathcal{U}\left(z^-, z^+\right), \end{aligned} \tag{13}$$

where $\mathcal{U}(\alpha, \beta)$ denotes the uniform distribution with lower limit α and upper limit β.

4. Checking if at least one sample fulfills all ellipsoidal inequalities

In this last step, we verify whether a determined sample x_j fulfills the ellipsoidal inequalities given by:

$$\left(x_j - \mu_i\right)^{\mathrm{T}} \Sigma_{\hat{x}_i}^{-1} \left(x_j - \mu_i\right) \leq 1 \quad \forall\, i \in \{1, \ldots, s\}. \tag{14}$$

Once a sample is found that fulfills all inequalities, we have proven that all ellipsoids are intersecting in at least one point.

V. RESULTS

In this section, we show the benefit of the proposed method. We consider the exemplary error ellipsoids depicted in Fig. 3. The two left error ellipsoids are equal in all four subfigures. The right error ellipsoid of subfigure (a) is scaled by $\alpha = \{1.25, 1.5, 1.75\}$ in the other subfigures. The figures also include the CTRBB as red box, which is mostly hidden behind the error ellipsoids. The three error ellipsoids have a common intersection in subfigures (b), (c) and (d) but not in subfigure (a). The CTRBB exists despite the absence of an intersection of all three ellipsoids. This shows the need of the fourth step of our methodology.

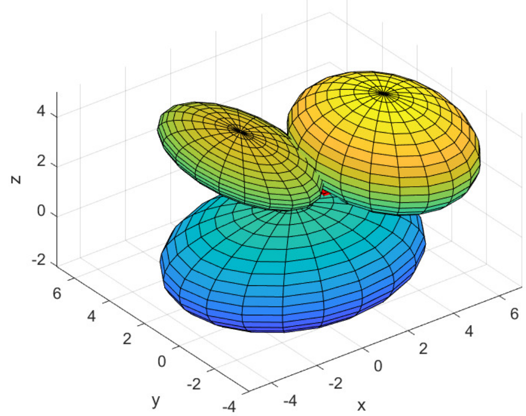

(a) $\alpha = 1.00$

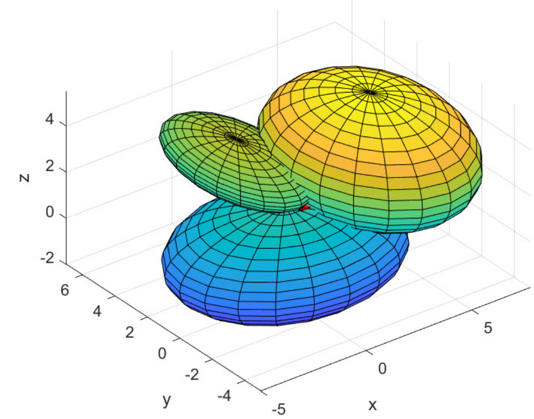

(b) $\alpha = 1.25$

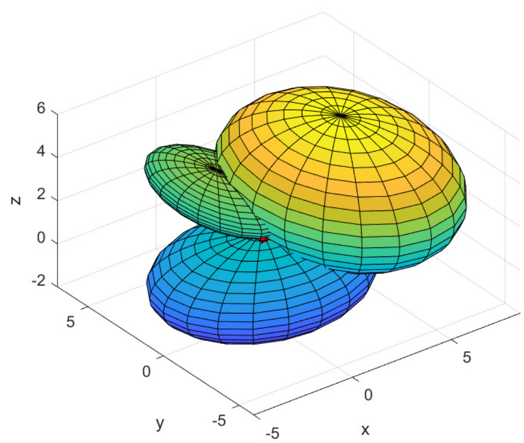

(c) $\alpha = 1.50$

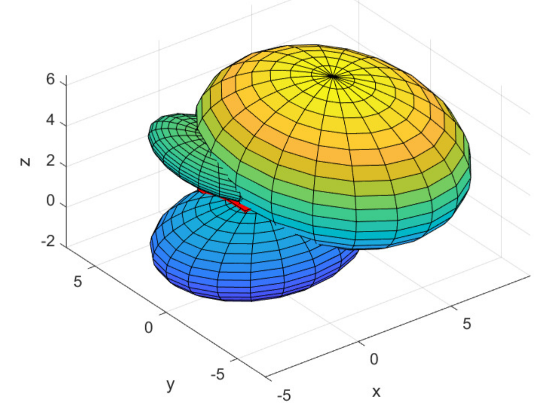

(d) $\alpha = 1.75$

Figure 3: Exemplary error ellipsoids from three different positioning sensors. The two left error ellipsoids are equal in all four subfigures. The right error ellipsoid of subfigure a is scaled by $\alpha = \{1.25, 1.5, 1.75\}$ in the other subfigures. Each figure also includes the CTRBB as red box, which is mostly hidden behind the ellipsoids. The 3 ellipsoids have a common intersection in subfigures (b), (c) and (d) but not in (a).

The number of uniformly distributed samples needed to find the intersection of the 3 ellipsoids is the key parameter for analyzing the efficiency of the method. We consider the error ellipsoids of Fig. 3 and use a maximum of 10^4 samples, i.e. "no intersection" is declared after having tested 10000 samples without finding an intersection point.

We compare the sampling of the CTRBB with the sampling of the individual bounding boxes. For the latter one, we have split the number of samples equally over all individual bounding boxes. Fig. 4 shows the obtained result: Our proposed method reduces the required number of samples by nearly two orders of magnitude for the mid-range values of $\alpha = \{1.25, 1.50\}$. For $\alpha = 1$, both approaches tested 10^4 samples due to the lack of any common intersection point. However, a smaller number of samples would be sufficient for the CTRBB as its volume is much smaller than the one of the individual bounding boxes. For very large values of α, the benefit of the proposed method also reduces as the size of the intersection area increases. Nevertheless, the proposed method is numerically very attractive as the medium range of α is practically very relevant.

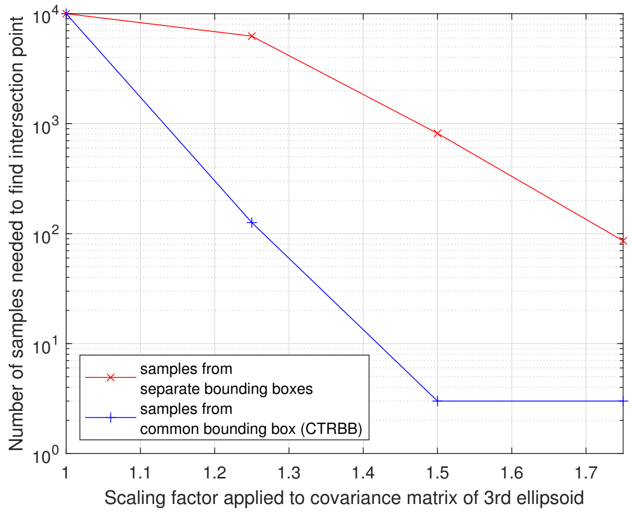

Figure 4: Number of samples needed to find intersection point for three exemplary error ellipsoids.

VI. DISCUSSION AND CONCLUSIONS

In this paper, we have provided a methodology for checking the intersection of error ellipsoids from at least two independent positioning sensors. We believe that our approach is in particular helpful for three or more sensors as there is no analytical solution available for these cases. The proposed method is numerically much more efficient than a brute-force sampling of the individual error ellipsoids or there bounding boxes. The typical application of the method is the pre-processing for improving the single sensor covariance matrices. Thereby, it is highly relevant as most sensor fusion algorithms (e.g. least-squares, Kalman filter) fully rely on a correct knowledge of the statistics.

The proposed method can be applied to both positioning and attitude determination. In both cases, carrier phase integer ambiguities need to be resolved to achieve a high accuracy. The ambiguity resolution related to attitude determination is typically more reliable than for positioning as it uses prior information on the baseline length. It can be further enhanced by including prior information on the baseline attitude as described by Henkel and Günther (2012).

The proposed method also has some limitations: The error ellipsoids are characterized by a mean value and a covariance matrix. The mean value refers to the bias of the sensor and was assumed to be known in this paper. However, it needs to be estimated or at least verified as well. Moreover, different sensors typically operate in different coordinate frames and the related transformations depend on the orientation of the object.

ACKNOWLEDGEMENTS

The authors would like to thank the German Federal Ministry for Economics and Climate Action (BMWK) for a grant to the project "SafeADArchitect" (grant number: 19A20013D), in which ANavS develops a risk-sensitive positioning system and real-time capable positioning methods for safeguarding of automated vehicles.

REFERENCES

Alfano, S. and Greer, M. (2003). Determining If Two Solid Ellipsoids Intersect. *Journal of Guidance, Control and Dynamics*, 26(1):106–110.

Brown, R. and Hwang, P. (2012). *Introduction to Random Signals and Applied Kalman Filtering with Matlab Exercises*. Wiley, New York.

Duzak, J. (2007). Lecture notes on Intersection Detection of Two Ellipsoids, paul g. allen school of computer science and engineering.

Gilitschenski, I. and Hanebeck, U. (2012). A robust computational test for overlap of two arbitrary-dimensional ellipsoids in fault-detection of kalman filters. In *Proc. of the 15th Int. Conf. on Information Fusion (Fusion 2012)*, pages 396–401, Singapore.

Henkel, P. and Günther, C. (2012). Reliable Integer Ambiguity Resolution: Multi-frequency Code Carrier Linear Combinations and Statistical A Priori Knowledge of Attitude. *Navigation*, 59(1):61–75.

Henkel, P., Iafrancesco, M., and Sperl, A. (2016). Precise Point Positioning with Multipath Estimation. In *Proc. of ION/ IEEE Position, Location and Navigation Symposium (PLANS)*, pages 144—-149, Savannah, Georgia, USA.

Henkel, P. and Sperl, A. (2016). Precise RTK Positioning with GPS/ INS Tight Coupling and Multipath Estimation. In *Proc. of ION International Technical Meeting*, pages 1015–1023, Monterey, CA, USA.

Kerr, T. (1974). A two ellipsoid overlap test for real time failure detection and isolation by confidence regions. In *Proc. of IEEE Conference on Decision and Control including the 13th Symposium on Adaptive Processes*, pages 735–742, Phoenix, AZ, USA.

Leonard, J. and Durrant-Whyte, H. (1991). Simultaneous map building and localization for an autonomous mobile robot. In *Proc. of IEEE/RSJ Int. Workshop on Intelligent Robots and Systems (IROS)*, volume 3, pages 1442–1447, Osaka, Japan.

Murty, K. (2000). *Linear Programming*. Wiley, New Jersey.